2019

MORPHOLOGY CHANGES TO CARMEL RIVER STATE BEACH IN RELATION TO WAVES AND RIVER DISCHARGE

Coughlin, Jillian N.

Monterey, CA; Naval Postgraduate School

NAVAL POSTGRADUATE SCHOOL

MONTEREY, CALIFORNIA

THESIS

MORPHOLOGY CHANGES TO CARMEL RIVER STATE BEACH IN RELATION TO WAVES AND RIVER DISCHARGE

by

Jillian N. Coughlin

June 2019

Thesis Advisor:	Mara S. Orescanin
Second Reader:	Edward B. Thornton

THIS PAGE INTENTIONALLY LEFT BLANK

REPORT DOCUMENTATION PAGE			Form Approved OMB No. 0704-0188

1. AGENCY USE ONLY *(Leave blank)*	2. REPORT DATE June 2019	3. REPORT TYPE AND DATES COVERED Master's thesis

4. TITLE AND SUBTITLE
MORPHOLOGY CHANGES TO CARMEL RIVER STATE BEACH IN RELATION TO WAVES AND RIVER DISCHARGE

5. FUNDING NUMBERS

6. AUTHOR(S) Jillian N. Coughlin

7. PERFORMING ORGANIZATION NAME(S) AND ADDRESS(ES)
Naval Postgraduate School
Monterey, CA 93943-5000

8. PERFORMING ORGANIZATION REPORT NUMBER

9. SPONSORING / MONITORING AGENCY NAME(S) AND ADDRESS(ES)
N/A

10. SPONSORING / MONITORING AGENCY REPORT NUMBER

11. SUPPLEMENTARY NOTES The views expressed in this thesis are those of the author and do not reflect the official policy or position of the Department of Defense or the U.S. Government.

12a. DISTRIBUTION / AVAILABILITY STATEMENT
Approved for public release. Distribution is unlimited.

12b. DISTRIBUTION CODE
A

13. ABSTRACT (maximum 200 words)

Morphological changes to beaches are the result of sediment transport via wind forcing, water flow, and human interference. Extreme morphological change to beaches occurs when a breach occurs across a beach. Each year, an ephemeral river breaches Carmel River State Beach (CRSB), a pocket beach that separates Carmel Bay from Carmel River, after lagoon water levels reach a certain height. Some seasons have a breach located constantly at the southern end of CRSB. During other years, the river breach migrates to the north throughout the season prior to relaxing to the south for breach closure. Using aerial photography and Structure from Motion photogrammetry, this study investigates the seasonal movement of the ephemeral river channel across the beach, the effects of wave height and direction on the morphological changes observed, and the overall net transport of sediment involved from December 2016 to June 2018. CRSB was found to be a closed system of sediment transport due to alternating migratory and stationary breach seasons. Migratory years cause beach erosion while stationary years yield sediment accretion or beach building, creating a stabilizing effect on the long-term sediment balance of CRSB. Findings suggest that river breach migration at CRSB is influenced by river discharge levels and local wave climate. In the wave climate at CRSB, there are slight seasonal variations in wave direction that result in enhanced northward momentum during migratory years.

14. SUBJECT TERMS
Carmel, beach morphology, breach, river, wave height, topography, SfM, Structure from Motion, Carmel River State Beach, aerial photography, photogrammetry, migratory, river discharge

15. NUMBER OF PAGES
61

16. PRICE CODE

17. SECURITY CLASSIFICATION OF REPORT	18. SECURITY CLASSIFICATION OF THIS PAGE	19. SECURITY CLASSIFICATION OF ABSTRACT	20. LIMITATION OF ABSTRACT
Unclassified	Unclassified	Unclassified	UU

NSN 7540-01-280-5500

Standard Form 298 (Rev. 2-89)
Prescribed by ANSI Std. 239-18

THIS PAGE INTENTIONALLY LEFT BLANK

Approved for public release. Distribution is unlimited.

MORPHOLOGY CHANGES TO CARMEL RIVER STATE BEACH IN RELATION TO WAVES AND RIVER DISCHARGE

Jillian N. Coughlin
Lieutenant, United States Navy
BS, U.S. Naval Academy, 2014

Submitted in partial fulfillment of the
requirements for the degree of

MASTER OF SCIENCE IN METEOROLOGY AND PHYSICAL OCEANOGRAPHY

from the

NAVAL POSTGRADUATE SCHOOL
June 2019

Approved by: Mara S. Orescanin
Advisor

Edward B. Thornton
Second Reader

Peter C. Chu
Chair, Department of Oceanography

THIS PAGE INTENTIONALLY LEFT BLANK

ABSTRACT

Morphological changes to beaches are the result of sediment transport via wind forcing, water flow, and human interference. Extreme morphological change to beaches occurs when a breach occurs across a beach. Each year, an ephemeral river breaches Carmel River State Beach (CRSB), a pocket beach that separates Carmel Bay from Carmel River, after lagoon water levels reach a certain height. Some seasons have a breach located constantly at the southern end of CRSB. During other years, the river breach migrates to the north throughout the season prior to relaxing to the south for breach closure. Using aerial photography and Structure from Motion photogrammetry, this study investigates the seasonal movement of the ephemeral river channel across the beach, the effects of wave height and direction on the morphological changes observed, and the overall net transport of sediment involved from December 2016 to June 2018. CRSB was found to be a closed system of sediment transport due to alternating migratory and stationary breach seasons. Migratory years cause beach erosion while stationary years yield sediment accretion or beach building, creating a stabilizing effect on the long-term sediment balance of CRSB. Findings suggest that river breach migration at CRSB is influenced by river discharge levels and local wave climate. In the wave climate at CRSB, there are slight seasonal variations in wave direction that result in enhanced northward momentum during migratory years.

THIS PAGE INTENTIONALLY LEFT BLANK

TABLE OF CONTENTS

THIS PAGE INTENTIONALLY LEFT BLANK

LIST OF FIGURES

THIS PAGE INTENTIONALLY LEFT BLANK

LIST OF TABLES

THIS PAGE INTENTIONALLY LEFT BLANK

LIST OF ACRONYMS AND ABBREVIATIONS

CDIP	Coastal Data Information Program
CRSB	Carmel River State Beach
GCP	Ground Control Point
LiDAR	Light Detection and Ranging
MOP	Monitoring and Prediction
MPWMD	Monterey Peninsula Water Management District
RMSE	Root Mean Square Error
SfM	Structure from Motion
SMS	Surface-water Measuring Software
UAS	Unmanned Aerial System
USGS	United States Geological Survey

THIS PAGE INTENTIONALLY LEFT BLANK

ACKNOWLEDGMENTS

Throughout this process, many people have supported me with guidance, data collection, and processing power. I wish to take the time to thank a few key participants.

I would like to thank Dr. Mara Orescanin for her time and effort in guiding me through this thesis project and process. From answering endless questions, conducting field work, and providing an amazing work environment, you have been a superb thesis advisor and a wonderful mentor.

Thank you, Dr. Edward Thornton, my second reader, for providing additional resources and another perspective when reviewing my project. You brought so much experience to the table. I also would like to acknowledge the following:

- To Jeremy Metcalf for his endless Photoscan assistance and point cloud instruction. I could not have completed half the analysis I did without this guidance
- To Paul Jessen for his knowledge in collecting GPS markers and conducting beach surveys
- To Jon Warrick and Andy Ritchie with U.S. Geological Survey team for providing the images of Carmel River State Beach for this project, river data to analyze environmentals, and clarification on questions that arose
- To Richard Lind for assistance in gathering precipitation data and Steve Anderson, National Weather Service San Francisco/Monterey Bay Area Observation Program Leader, for providing the local rainfall data in Carmel-by-the-Sea
- To CDR Travis and all the professors and staff at Naval Postgraduate School for supporting me through my studies and making graduate school an adventure

My cohort deserves an extra special thank you for providing laughter and support throughout this entire process. Thanks for being a second family for me here at school!

Finally, thank you to my family and fiancé for their love and support!

THIS PAGE INTENTIONALLY LEFT BLANK

I. MOTIVATION

The Navy and Marine Corps operate in remote locations where there is often an inability to conduct traditional full GPS surveys, whether due to the amount of initial personnel on the ground, timing of mission, or cost of equipment. Specifically, the Marine Corps conducts amphibious, or beach, landings in both training evolutions and real-world operations. The success of beach landings is largely determined by sediment cohesion and compaction on the beach. Sediment cohesion describes the stability of the attraction between sediment molecules and compaction refers to the density of grain packing (Dean and Dalrymple 2002). If there is consistent or frequent transport of sediment and changes to the beach shape, the sediment will have lower compaction and will not support as much weight without deforming. When this occurs, large equipment, such as vehicles or tanks, will sink and become lodged in the sand. Based on this information, basic photographs of the beach landing location can be misleading.

The focus of this study is to determine how aerial photographs of remote locations could be used to measure the suitability of a location as a landing site. Structure from Motion (SfM) photogrammetry combines aerial photographs to create elevation maps. If this approach proves to be accurate, this could allow the military to quickly detect changes to topography over time, the opening of ephemeral rivers, or movement of river access through the use aerial photography from drones to create 3-D topography maps of secluded areas. Furthermore, this approach could also be used when the Navy responds to Humanitarian Assistance and Disaster Relief operations or simply as a remote sensing tool.

THIS PAGE INTENTIONALLY LEFT BLANK

II. INTRODUCTION

Beach morphology is driven by the transport of sediment from one location to another, resulting in change to the given topography of an area. Sediment can be moved via wind forcing, water flow, or human interference. Sediment on beaches can be transported by water during the occurrence of breaking waves through seaward transport (caused by wave undertow) or shoreward transport (caused by overwash) (Jiménez 2007). Sediment that is transferred within a river body changes the shape of not only the river, but also the beach and berms surrounding the river, while potentially changing the sediment composition (Wolman 1967; Kench 1999; Komar 1998; Aubrey and Speer 1984; Scooler 2017; Young 2018). Sediment movement can cause variations in elevation, changes in beach slope gradients, or erosion of sediment (Rich and Keller 2013; Bascom 1953; Komar 1998; Jiménez 2007).

Some of the most dynamic or varying beach systems exist around ephemeral rivers (also known as bar built estuaries). Ephemeral rivers are characterized by varying flow intensity, largely driven by seasonal precipitation rates. Ephemeral rivers, similar to tidal inlets, migrate, create new channels, and episodically breach through barriers prior to reaching an outlet (Behrens et al. 2009). A breach is defined as a narrow opening within a landmass that enables water to flow between two separate bodies of water (Kraus et al. 2002). Commonly, breaches reduce water levels within a lagoon or marshland to avoid flooding in surrounding areas and to allow for the migration of marine life (Kraus et al. 2002; Scooler 2017). Opening the backwater lagoon to waves from the bay or ocean facilitates exchange of water between the two water bodies and sometimes results in changes to the salinity of the lagoon (Kraus et al. 2002). Breaches can occur both naturally and manually (Kraus et al. 2002; Behrens et. al 2013). Natural breaches occur when high backwater lagoon levels cause the lagoon water to scour through the beach or when seepage through porous sediment creates a lead (Pierce 1970; Kraus et al. 2002; Kraus and Wamsley 2003; Scooler 2017). Alternatively, manual or artificial breaches are created when channels are artificially dug across a barrier (Kraus et al. 2002; Orescanin et al. 2019). Artificial channels are generally created to avoid

flooding in suburban areas. These man-made channels can result in insufficient flow or early breach closure due to insufficient water build up to maintain the outlet (Kraus and Wamsley 2003; Young 2018). Breach closures occur when consistently high tides or very high waves build up sand at the opening of an outlet (Pierce 1970; Behrens et al. 2009; Orescanin and Scooler 2018). Furthermore, the shape of the outlet can determine the probability of breach closure: straight outlets have low probability while curved outlets have higher probability due to increased surface area (Behrens et al. 2009; Orescanin and Scooler 2018). Hydraulic parameters, such as wave height, limit closure events occurring on the tidal scale (Behrens et al. 2013).

Full topographical surveys are difficult, time-consuming, and costly to conduct. Thus, not many studies evaluate ephemeral rivers, especially smaller ones (Carrivick et al. 2013). In 2013, Carrivick et al. delineated several modern techniques to collect the survey data required to evaluate topographical changes: GPS, Light Detection and Ranging (LiDAR), and Structure from Motion (SfM) photogrammetry. GPS and LiDAR are efficient, but can require long collection times and have high associated costs (Carrivick et al. 2013). SfM represents a faster, cost-effective method of creating the required datasets for observing changes to elevation at specific locations (Carrivick et al. 2013; Westoby et. al. 2012). Using overlapping photos taken at any angle, SfM estimates the camera position and meshes together similar terrain features in the photographs to create a point cloud of images (Snavely et al. 2008; Westoby et al. 2012). One caveat to this technique is that images with low textural diversity yield less accurate results in SfM (Fonstad et al. 2012). Ground control points (GCPs) are subsequently used to tie the point cloud into a coordinate system and create a dense point cloud (Westoby et al. 2012).

This study examines the morphological evolution of Carmel River, an ephemeral river located in central California, over two contrasting winter seasons. Separated from Carmel Bay by the Carmel River State Beach (CRSB) (Figure 1), the Carmel River seasonally breaches into the bay most years, causing topographic changes to the shape of the beach based on the initial location of the breach and the meanderings of the outlet after breaching (Kraus et al. 2002; Kraus and Munger 2008; Scooler 2017; Young 2018; Orescanin and Scooler 2018). Using aerial photography and the implementation of SfM

photogrammetry, this study aims to determine the existence of a pattern within the seasonal migration of the breach along the beach.

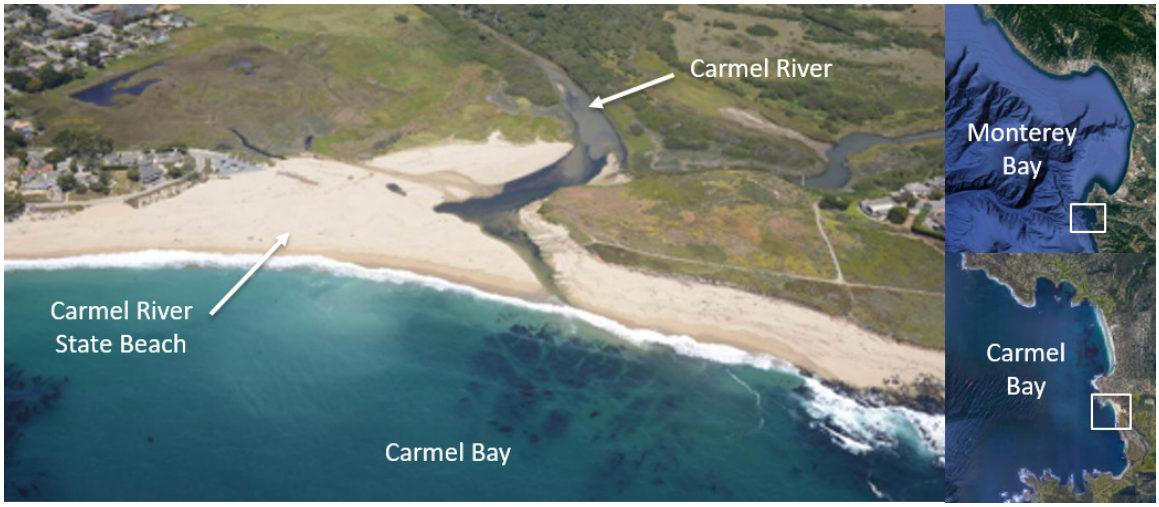

Figure 1. Carmel River State Beach location

The study period examines two subsequent breach seasons of the Carmel River: December 2016 to June 2017 and December 2017 to June 2018. During the first year, the breach initializes at the southern end of the beach, slowly migrates to the north from January to March, and then relaxes to the south for breach closure. This year saw higher rainfall than usual for the area. The following year (2017–2018), the breach formed at the southern end of the beach in early winter and remained in the same position for the duration of the breach season.

Owing to the long-term (decadal) stability at Carmel River State Beach (Figure 2), it is possible to study short-term breaching events and migrations over many years without the need to consider longer scale migrations. Traditionally, beaches tend to aggregate or erode through sediment transport and migration. However, as seen in Figure 2, this beach has historically maintained a similar width and length extent. The breaching by the Carmel River occasionally results in migration of the river outlet on the scale of hundreds of meters, effectively altering the beach profile.

Past research of this system investigated the momentum balances between the lagoon discharge and ocean forcing, noting that breaches will occur during periods of increased discharge with constant ocean forcing and periods of constant discharge with decreased ocean forcing (Scooler 2017, Orescanin and Scooler 2018). In 2018, Young found that SfM is an effective way to measure beach morphology when data does not involve working with submerged areas. Reflection and refraction caused the SfM measurements over submerged surfaces to often be inaccurate (Young 2018). Additionally, Rich and Keller (2013) performed model runs which demonstrated that breaches are generally controlled by discharge, or streamflow, and overtopping. Of these two methods, overtopping driven breaches are usually "short-lived" when compared to streamflow driven events (Rich and Keller 2013). Furthermore, this study stated that decreased lagoon berm heights in the model allow for increased wave overtopping to occur while increasing the water elevation of the lagoon required to effectively breach the berm (Rich and Keller 2013).

These images were generated using Google Earth.

Figure 2. Historical comparison of Carmel River State Beach extent and shape in 1998 (left) and 2018 (right)

An additional objective of this study is to establish whether the migration of the river channel (and subsequent sediment transport) is an effect of river discharge or wave height and direction. There is little research regarding migration of ephemeral rivers. For tidal inlets, Aubrey and Speer (1984) found that there were three main processes causing

updrift migration of the inlet at Nauset Inlet, a tidal inlet in Massachusetts opening directly to the Atlantic Ocean. These processes included accretion of ebb tidal delta bars due to longshore sediment transport, storm-induced shifts, and ebb tide discharge around the inlet channel bend (Aubrey and Speer 1984). Of these methodologies, only ebb tidal delta bar accretion occurred on a time scale of months, whereas the other two methods were observed to have a decadal reoccurrence or episodic effects (Aubrey and Speer 1984). This time scale matches the seasonal variations that are observed with the Carmel River breach. The Carmel River breach is sheltered within Carmel Bay and is generally affected by wave directions between 280–300 degrees (James 2005). Following initial opening, the breach, historically, will remain open 85% of the season prior to final closure (James 2005). The location of the breach was observed to form an elongated outflow to the north or south approximately 50% of the time between 1991 and 2005 (James 2005). This elongation was hypothesized to be related to swell direction and overarching ocean conditions (James 2005), but there has not been further research into this area.

The hypothesis of this study regarding what causes the variation in river breach migration for Carmel River is that breach movement is largely driven by river discharge and berm height, but the phenomenon can be affected by large waves from storm events. This hypothesis is tested through analysis of aerial imagery and physical data (wave heights, wave direction, tides, water level, precipitation, and discharge rates) for two breach seasons at Carmel River State Beach. The aerial imagery allows for the analysis of beach elevation and subsequent sediment movement throughout the season while the physical data provides a sufficient overview of area and processes effecting it.

THIS PAGE INTENTIONALLY LEFT BLANK

III. METHODOLOGY

Beach elevation surveys were conducted from December 2016 through September 2018 with flights by the United States Geological Survey (USGS) team and by an unmanned aerial system (UAS). These surveys span two seasons of barrier breaching and are used to determine the presence of morphological changes to the beach topography from month to month. All surveys required GPS-realized ground control points (GCPs) to tie the images to a reference coordinate system. This study used the WGS-84 reference system and an Ashtech ProMark GPS receiver was used to record the location of GCPs. GCP locations were surveyed for at least 5 minutes to obtain accurate measures (Figure 3).

Figure 3. GPS positioning of a ground control point

A. USGS SURVEY

The USGS team flew surveys of Carmel River State Beach using a Nikon D800 and a Nikon D810 mounted to a fixed-wing aircraft (Cessna 182) with a GPS antenna. Both cameras operated at 36.3-megapixel resolutions and took pictures of the Carmel River State Beach at an oblique angle. The Nikon D800 camera used various focal lengths in flight (50mm, 30mm, and 40mm) and the Nikon D810 used a focal length of

40mm. These photographic surveys were conducted each month during the 2017 breach season (December 2016 through June 2017). The following year, there were five surveys conducted during the 2018 breach season (December 2017, January 2018, March 2018, May 2018, September 2018). The aircraft-produced images covered a large frame of view and each survey consisted of 37 to 52 images.

The USGS surveys did not use pre-positioned, study-specific GCPs. Fourteen GCPs were identified within the photographs and precise GPS of the GCPs was measured during fieldwork with the Ashtech ProMark. These GCPs consisted of high-contrast, easily identifiable features such as pothole covers, road markings, fence corners, signposts, and an elementary school foursquare court. The Root Mean Square Error (RMSE) given in centimeters for the USGS GCPs and supporting check points are provided in Table 1 and Table 2, respectively. The total error for both the GCPs and check points is similar.

Table 1. USGS GCP root mean square error: x-longitude, y-latitude, z-altitude

Survey Date	Number of GCPs	X error (cm)	Y error (cm)	Z error (cm)	XY error (cm)	Total (cm)
05/19/2017	12	33	37	16	50	53

Table 2. USGS check point root mean square error: x-longitude, y-latitude, z-altitude

Survey Date	Number of Check Points	X error (cm)	Y error (cm)	Z error (cm)	XY error (cm)	Total (cm)
05/19/2017	2	33	20	7.5	39	39

B. UAS SURVEY

Using the same UAS camera parameters and flight patterns outlined in Young's 2018 work, a DJI Phantom III Advanced quadcopter (Figure 4), was flown over the

Carmel River, beach, and surrounding areas to conduct a survey of terrain elevation. The collection dates in this study build on Young's (2018) previous surveys of December 06, 2017, January 10, 2018, and January 23, 2018. This study incorporates a closed breach in February 28, 2018 and a secondary opening observed on May 17, 2018.

Figure 4. DJI Phantom III Advanced quadcopter

Each survey date using the UAS had specific GCPs that were placed and measured during the flight. The GCPs used during the UAS surveys were 2.5-foot by 2.5-foot plywood boards painted with black and natural quad panels to allow for maximum contrast in aerial viewing. These GCPs were placed on the beach and in the immediate area. The UAS RMSE values are given in Table 3 and Table 4 for the GCPs and check points, respectively.

Table 3. UAS GCP root mean square error: x-longitude, y-latitude, z-altitude

Survey Date	Number of GCPs	X error (cm)	Y error (cm)	Z error (cm)	XY error (cm)	Total (cm)
12/06/2017	5	2.8	3.3	23	4.3	23
01/10/2018	4	2.5	4.8	4.0	5.5	6.8
01/23/2018	10	2.9	7.3	11	7.8	13
02/28/2018	9	1.1	2.5	29	3.1	29
05/17/2018	4	2.0	2.0	4.0	3.2	5.1

Table 4. UAS check point root mean square error: x-longitude, y-latitude, z-altitude

Survey Date	Number of Check Points	X error (cm)	Y error (cm)	Z error (cm)	XY error (cm)	Total (cm)
12/06/2017	1	1.9	5.3	36	5.6	36
01/10/2018	1	1.1	2.9	4.0	3.1	5.1
01/23/2018	2	5.1	5.0	2.3	7.2	7.5
02/28/2018	2	8.1	13	34	16	37
05/17/2018	1	1.3	3.8	8.6	4.0	9.5

C. WAVE HEIGHTS AND WAVE HEIGHT GRADIENTS

Directional wave spectra measured every hour at the offshore National Data Buoy Center (NDBC) Station 46239 are refracted shoreward to the 15-meter isobaths approximately every 200 meters alongshore in Carmel Bay at the Monitoring and Prediction sites (MOPs) as provided by Coastal Data Information Program (CDIP). The directional spectra at the MOP sites were integrated to obtain wave height (Figure 10 and Figure 11) and radiation stress values (Figure 15). These datasets were verified and validated by the CDIP Program using MOP v1.1 validation datasets and Datawell's spectra layout with initialization parameters for both northern and southern California (Coastal Data Information Program 2016). The coordinates and locations of the six sites can be found in Figure 5 and Table 5. The datasets provide wave height, direction, period, and radiation stress from December 2016 through June 2018.

The stations plotted measure lagoon level, river discharge, and precipitation rates. The CDIP MOP sites are located along the 15-meter isobaths at Carmel River State Beach.

Figure 5. Data site locations

For comparison with historical observations, a NDBC dataset from the Point Sur buoy, located at 36°20'34" N 122°5'45" W, provided wave height and direction from December 2016 through June 2018 every 30 minutes (NOAA NDBC 2019). These values were compared to the CDIP hindcast data to observe how wave height and direction changes as the waves travel into Carmel Bay. Wave height and direction were plotted for each MOP location for the duration of the season (Figure 10 and Figure 11).

Table 5. CDIP MOP and precipitation station locations

	Latitude	**Longitude**
CDIP Buoy		
MO630	36.53057098388672	-121.9300765991211
MO631	36.5319709777832	-121.93150329589844
MO632	36.534149169921875	-121.93229675292969
MO633	36.53559112548828	-121.93328094482422
MO635	36.535579681396484	-121.93382263183594
MO636	36.53776931762695	-121.93631744384766
	Latitude	**Longitude**
Precipitation Station		
Site 210 / CML	36.540889	-121.88196
EW6019 / CRM	36.55150	-121.92583

By interpolating the wave height data to the same time scales, wave height differences between the Point Sur and CDIP MOPs were calculated and plotted over time, colored by wave direction. This plot (Figure 13) will allow comparison of the offshore and onshore waves. To observe the wave height gradient along the coast, the difference between one northern CDIP MOP site (MO635) and one southern CDIP MOP site (MO632) was plotted over time (Figure 12).

D. RIVER AND ENVIRONMENTAL DATASETS

River discharge and lagoon level datasets were obtained from Monterey Peninsula Water Management District (MPWMD). River discharge was measured in cubic meters per second and lagoon water level was given in meters every fifteen minutes from December 2016 through June 2018. The discharge was measured at the HWY 1 bridge over the Carmel River.

Hourly tidal data for Carmel Bay was collected from NOAA Tides and Currents Station 9413450, located at 36°36.3'N 121°53.3'W in Monterey Bay. This data provides the water level in meters, NAVD88.

Precipitation accumulation was provided by the Citizen Weather Observing Program (CWOP) and California Irrigation Management Information System (CIMIS) at two weather stations in the Carmel area. Station locations can be found in Table 5 and Figure 5. Site 210 (CML) is located in Carmel Valley, CA, while EW6019 (CRM) is located in downtown Carmel-by-the-Sea, CA. Site 210 (CML) and EW6019 (CRM) sample rain accumulation every hour and every fifteen minutes, respectively.

Combined with the wave height data, these parameters were analyzed and compiled into a composite figure, described in Chapter V, to provide overviews of the region during the breach season.

E. DENSE CLOUD DESIGN

To measure the changes in elevation caused by sediment transport over time, a three-dimensional model of the beach elevation was created using SfM photogrammetry procedures for each survey flight. Overlapping photographs taken at various angles and

embedded with GPS coordinates were input into the SfM software, Agisoft Photoscan Professional version 1.4.1. SfM software matches and aligns similar features between the photographs and builds a sparse cloud of the collected data points (Snavely et al. 2008; Westoby et al. 2012). Aligned images are subsequently tied to a coordinate system using a set of GCPs for each image set, assigning XYZ values to the image pixels (Westoby et al. 2012; Young 2018). From here, a dense point cloud can be produced using the positioning data for the USGS and UAS survey flights (Westoby et al. 2012; Young 2018).

In this study, the USGS data were processed without an initial lens calibration. However, the UAS images used an initial lens calibration using the standard Photoscan process. Image alignment used high accuracy and adaptive camera model fitting enabled for all survey dates. The two projects (USGS and UAS) were kept separate by platform as the effects of varying the platform within the same project were yet unknown. Additionally, the photographs were taken at significantly different angles specific to their platform. USGS images were taken at largely oblique angles whereas all of the UAS data was shot top-down.

Due to the small number of photos in the USGS dataset, the key point and tie point limitations were adjusted to zero to allow for the highest quality alignment of the photos. One set of GCPs was used for all USGS survey dates. These GCPs canvassed the surrounding area and neighborhoods as the images from the aircraft covered a larger area. The GCPs were imported and individually placed for one survey date (May 19, 2017), saving two GCPs to use as check points. All USGS surveys were subsequently aligned to the May 19, 2017 survey to reduce human error introduced by individual GCP placement for each survey date.

Each UAS flight resulted in hundreds of photos for analysis. Following Young's (2018) procedure, the key point and tie point limits were set to 40,000 and 4,000 respectively. This optimized the time spent processing each image during alignment while still providing a high-quality result. Each UAS survey had date specific GCPs as the flight area was limited to the local beach area and GCPs had to be established on the beach itself via markers. These surveys were not aligned to one another.

The SfM software built dense point clouds for every survey date. All dense point clouds were designed to have “high” quality and “moderate” depth filtering. These dense clouds were converted to XYZ positioned data for each survey date.

F. CROSS-SECTION GENERATION AND COMPARISON

For ease of comparison, dense point cloud XYZ positioned data was exported from Photoscan in the WGS-84 UTM Zone 10N (ESPG:32610) coordinate system with the precision set to six decimal places. The XYZ points were imported to Aquaveo Surface-water Measuring Software (SMS) where it was interpolated to a 1-meter by 1-meter grid. These datasets act as elevation maps of the observed area for each survey date.

Figure 6. Carmel River State Beach cross-section locations

Seven shore-normal beach cross-sections were positioned across the beach to evaluate changes in beach elevation over time (Figure 6). These cross-sections were determined for each survey date, exported from SMS, analyzed and compared to other survey dates. Additionally, the differences between specific elevation maps were analyzed to observe the overall change in sediment movement, accretion or erosion, over

the course of the breach season. An example can be seen in Figure 7 where the seasonal elevation difference is depicted for both breach seasons utilizing the USGS point cloud data. These images allowed for greater analysis of where the sediment was most effectively being eroded, accreted, or deposited. Similarly, this process can be applied to individual survey dates, displaying of the effects of physical events that occurred between subsequent survey dates.

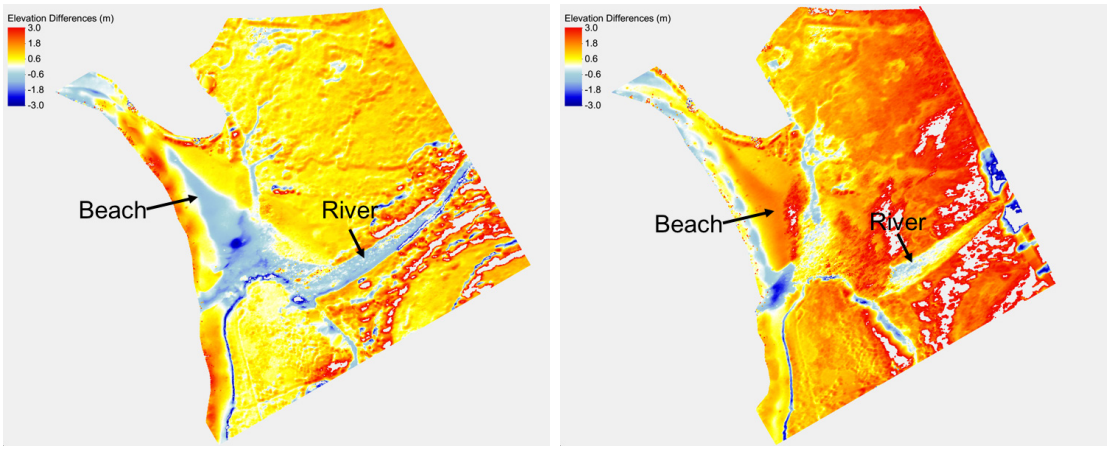

This figure displays elevation differences from December 20, 2016–June 26, 2017 (left) and December 21, 2017–May 28, 2018 season (right).

Figure 7. Seasonal elevation differences for USGS flights

THIS PAGE INTENTIONALLY LEFT BLANK

IV. BEACH MORPHOLOGY

A. RESULTS

Analysis of the photogrammetry surveys allowed for seasonal trends in morphology at CRSB to be established. Using the cross sections described in Figure 6, cross-shore elevation changes could be observed throughout each season. These results are displayed in Figure 8 and Figure 9.

1. 2016–2017 Breach Season

From the images taken by the USGS team and used to produce the cross-sections, it is established that the river outlet or breach migrated approximately 300 meters during the 2016–2017 breach season. The outlet starts at the southern end of the beach and slowly works its way to the northern end of the beach before returning to its original position. Figure 8 plots the cross-section elevations in meters (NAVD88) for each survey date and allows evaluation of the differences in elevation heights between the dates (i.e., how the beach is shifting).

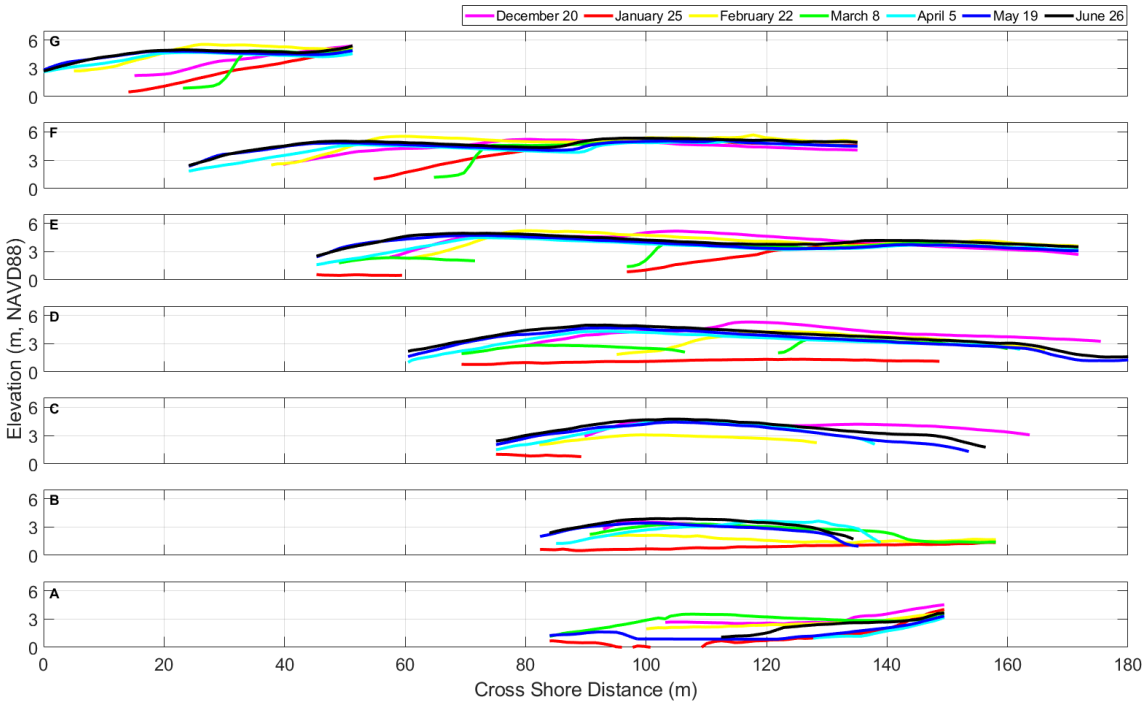

These profiles correspond with previous cross-sections found in Figure 6. The cross-sections are plotted from North to South.

Figure 8. USGS beach elevation cross-sections for the 2016–2017 breach season

Starting in December 2016, a relatively consistent beach elevation is seen throughout the cross-sections with the breach channel located toward the south. From December to January, there is an average beach elevation decrease of one to three meters along the fore beach. The River's initial breach occurred on December 12, 2016, at the southern end of the beach. This breach episodically closed a few times until January 3 when it stabilized and would remain open for the remainder of the season. By January 25, 2017, the river breach had evolved and established two outlet channels located in the center of the beach. By February, a significant accretion occurred in the foreshore at the northern end of the beach with moderate beach building occurring in the foreshore to the south. The breach shifted to the center of the beach. These data have been removed, as the camera is unable to accurately distinguish depths through water. In March, the breach channel migrates approximately 190 meters to the north where beach elevation is then observed to decrease by four meters. However, by April, the breach has shifted back to

the south and the northern beach elevations have rebuilt to four meters high. May and June see minimal change in the beach elevation profiles aside from some beach building occurring at the southern foreshore as beach closure approaches. The breach was observed closed after July 14, 2017 (Monterey Peninsula Water Management District 2017).

Throughout the entire breach season, the back beach from the center of the beach to the northern cross-sections (Figures 8E, 8F, 8G) remains at a relatively constant level. This is where the higher beach berm resides. The back beach in Figures 8C and 8D sees an erosion of about three meters in elevation throughout the season due to the breach cutting through the beach. However, this area is beginning to be rebuilt by the end of the season.

2. 2017–2018 Breach Season

In contrast to the previous season, the 2017–2018 breach season did not migrate from its initial breach location to the south. Consequently, the cross-sections for this season (Figure 9) show less variation between survey dates. The initial breach of this season was an artificial breach conducted by MPWMD on January 9, 2018. However, the breach was not stable and closed within a few days. The first natural breach occurred on January 21, 2018.

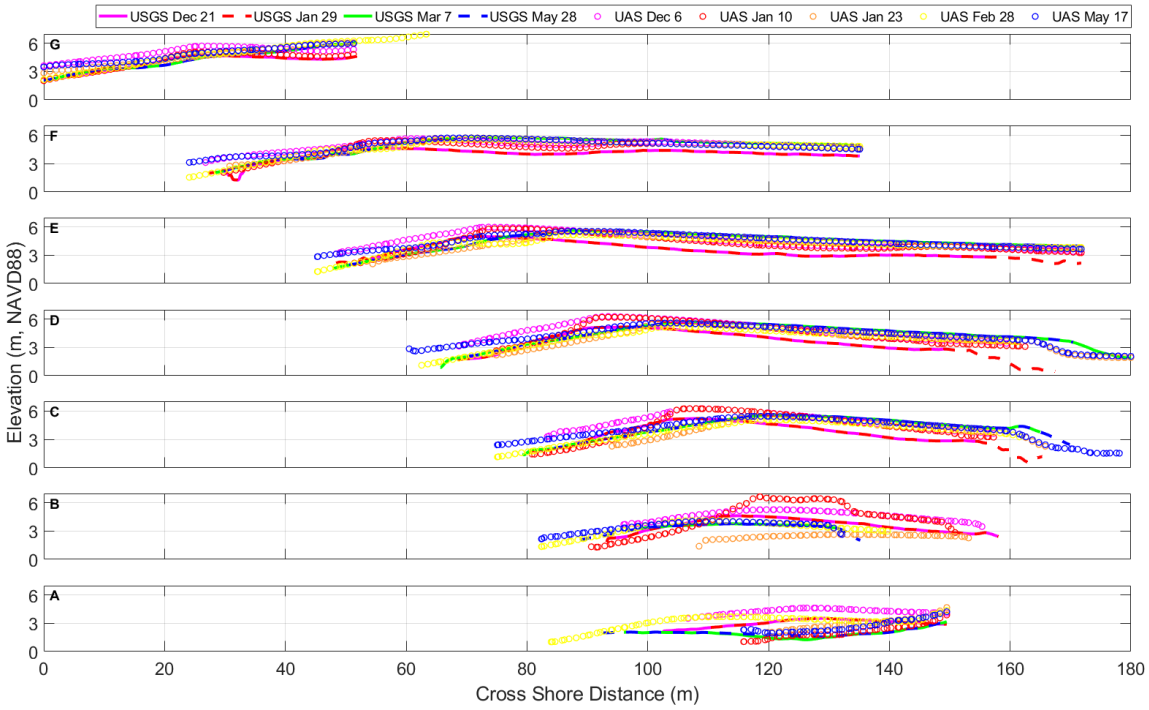

These profiles correspond with previous cross-sections found in Figure 6. The cross-sections are plotted from North to South. USGS data are delineated by lines and UAS data are delineated as circles.

Figure 9. Beach elevation cross-sections for the 2017–2018 breach season

From December to January, there is very little change across the beach. Between the January and March survey flights, the back beach elevation increased by one to two meters at the middle and northern portions of the beach (Figures 9C-G). Along the southern portion of the beach, additional areas of sand have been scoured down as the river cut through the beach. After these changes, the beach remains relatively the same shape until the May 28 flight. The breach was observed to be closed for the season after May 29, 2018 (Monterey Peninsula Water Management District 2018).

The beach elevations created via the UAS data agree with the elevations created using the USGS data (Figure 9). However, through surveying at various dates, the UAS data provide a more detailed examination of the 2017–2018 breach season. The largest contrast between USGS and UAS profiles are the changes in the upslope of the beach. In Figures 9C-E, the beach slope varies between survey dates. By the end of the season, the slope settles at a lower elevation than the start of the season. Furthermore, in Figure 9B,

there is evidence of the beach building between December and the start of January at the 120-meter cross-shore distance. This observation is not present in the USGS.

B. DISCUSSION

The beach cross-section measurements show two distinctly different morphological trends for two different years that help understand the historical stability of CRSB. During the 2016–2017 breach season (Figure 8), the beach undergoes large elevation changes at three specific sites via scouring and sediment accretion. First, in Figure 8D, by March, there is a clear display of the quantity of sand removed by river scouring as the river cuts through the beach to reach a northerly outlet. From December to March, the 110-meter cross-shore distance location decreases in elevation by approximately three meters. Second, the elevations change at the cross-shore position of 25–60 meters in Figure 8F. This site starts at an elevation of four meters in December and decreases to one meter by March due to river scouring. However, by the following June, the site has rebuilt to five meters in elevation. This change is due to onshore waves bringing sediment back to the beach once the river outlet relocates to the south of the beach. Ultimately, the upslope of the beach and berm height is being driven by the crest height of the consistent onshore waves. Third, during this migratory year, there are large changes to the back beach in the center of CRSB. In Figure 8C and 8D at cross-shore positions 130–180 meters, the back beach elevation begins the season at around four meters. This height falls throughout the season, but begins to build back up toward the end of the season when the breach repositions to the south. By June, back beach levels have increased to about three meters. However, the elevation does not return to the original height, suggesting a net loss of sand from the back beach.

The following year, the beach profile in December appears similar to how the previous season ended (Figure 9), which indicates little morphological evolution during prolonged periods of small waves and no river discharge. From December to January, there is minimal variation in the elevation heights. This may be occurring due to the episodic openings and closings of the channel during this time (Table 6). However, by March, the breach is stable and beach profiles display observable differences. To the

south near the outlet location (Figure 9A), river scouring removes sand from the beach resulting in a one to two meter decrease in beach elevation at the 130 meter cross-shore position. Conversely, on the back beach in Figures 9C and 9D, sediment accretion builds the beach and restores the beach elevation to its original height at the beginning of the previous season.

These findings suggest the following conclusions regarding the long-term stability at CRSB: (1) during migratory breach years, the beach height and back beach extent decreases as it is scoured away by the outlet channel; and (2) during stationary breach years, the beach begins to build back up where it had been eroded previously. From James (2005), fifty percent of the breach years at CRSB are migratory in nature. Due to the historical stability shown in Figure 2 and the observations of beach morphology, this study suggests that a reason CRSB is a cyclical or closed system for sediment transport is that there is a consistent series of migratory and stationary breach cycles.

The RMSE for this study is on the order of tens of centimeters with the majority of the error occurring in the z-direction. Error for the USGS flights was slightly higher than the values observed for the UAS flights. This variation in error could be caused by the height of the flight path as well as the angle of the camera when the image was taken. However, these RMSE values are comparable to the 40–60 centimeter RMSE found by Rich and Keller (2013) at CRSB. The observed changes in beach morphology in this study are on the order of meters, thus the observed error will not have a major impact on the findings as the RMSE is an order of magnitude smaller. Total volume of migrated sediment was not calculated because integrating over a ten centimeter error would induce huge errors in the calculation. Furthermore, with no bathymetry data, the sediment migration within the river outlet and offshore could not be accounted for.

V. ENVIRONMENTAL AND RIVER DATA

A. RESULTS

The environmental factors during the two observed breach seasons are shown in Figure 10 and Figure 11. Within the figures, Part A depicts wave height (in meters) and wave direction at the Point Sur buoy and several MOP sites, Part B shows river discharge levels (in cubic meters per second), Part C portrays the lagoon level and tidal data (in meters) over time, and Part D yields the hourly precipitation accumulation (in millimeters). The vertical lines within Part A represent the dates of aerial surveys conducted for this project. Black lines represent USGS survey dates and red lines represent UAS survey dates.

1. 2016–2017 Breach Season

From December 2016 to June 2017, the wave heights in Carmel Bay (observed via CDIP MOP sites) were relatively consistent between one to three meters with a few winter storm events exceeding three meters (Figure 10A). The wave heights from Point Sur were, on average, one to three meters larger than the waves inside Carmel Bay. A maximum wave height of ten meters was observed at the end of January. This observation is seen in the Point Sur data as well as at MO635. The value is delayed in the CDIP plot due to propagation time from Point Sur to MO635. Additionally, the data support that there is sheltering occurring at this location, largely due to the narrower aperture between Point Lobos and Carmel Point. There is a predominant wave direction at this location with the waves generally approaching from the west/northwest, varying in origin between 260–300 degrees.

River discharge (Figure 10B) appears negligible until the beginning of January where the discharge values begin to increase. The breach remained open for the majority of this observation season. Peak river discharge occurs in mid-February, increasing to 250 cubic meters per second. After this flow increase, the discharge levels begin to decrease and eventually dissipate as the river breach closes.

The lagoon water levels increased steadily until mid-December, peaking at 4.3 meters prior to the initial natural river breach forming (Figure 10C). Following this, the lagoon levels experienced a series of peaks as the breach stabilized itself, allowing water levels to increase in the lagoon prior to each subsequent breach. For the remainder of the season, the lagoon levels fluctuated between one to three meters elevation. Tides remain fairly constant throughout the season but are continuously at lower elevation than the lagoon water levels.

Finally, differences in precipitation along the coast (CRM) versus upstream in Carmel Valley (CML) show generally more rainfall observed along the coast (Figure 10D). Additionally, there is more frequent and higher accumulation precipitation events throughout January and February 2017.

2. 2017–2018 Breach Season

Wave heights from December 2017 to June 2018 are not as varied as the previous breach season, with fewer winter storm events (Figure 11A). The waves were consistently between one to four meters high in Carmel Bay. The largest wave height for this season is about six meters at the end of January, significantly lower than the previous year. The waves are observed to move in the same directions as the previous year. There is a slight increase in waves propagating from the north.

The river discharge levels (Figure 11B) are very low with the maximum for the season occurring at the end of March with a discharge flow of 70 cubic meters per second.

The lagoon levels (Figure 11C) are relatively higher at the start of this season at approximately 3.75 meters high, possibly due to the low discharge flow rate. On January 9, 2018, the river was manually breached to avoid flooding in the local area due to high lagoon levels. This breach is observed as the first significant drop in the lagoon level. However, the manual breach failed owing to lack of river discharge and the lagoon began to refill until it naturally breached itself approximately ten days later. Following this breach, the lagoon level is seen to oscillate throughout the remainder of the breach season until it begins to level off at the beginning of June.

Precipitation accumulation during this season (Figure 11D) is similar to the previous season. Again, the coastal area received higher levels of rain. Differing from the previous season, this figure portrays increased rain events toward the end of the breach season in March and April 2018.

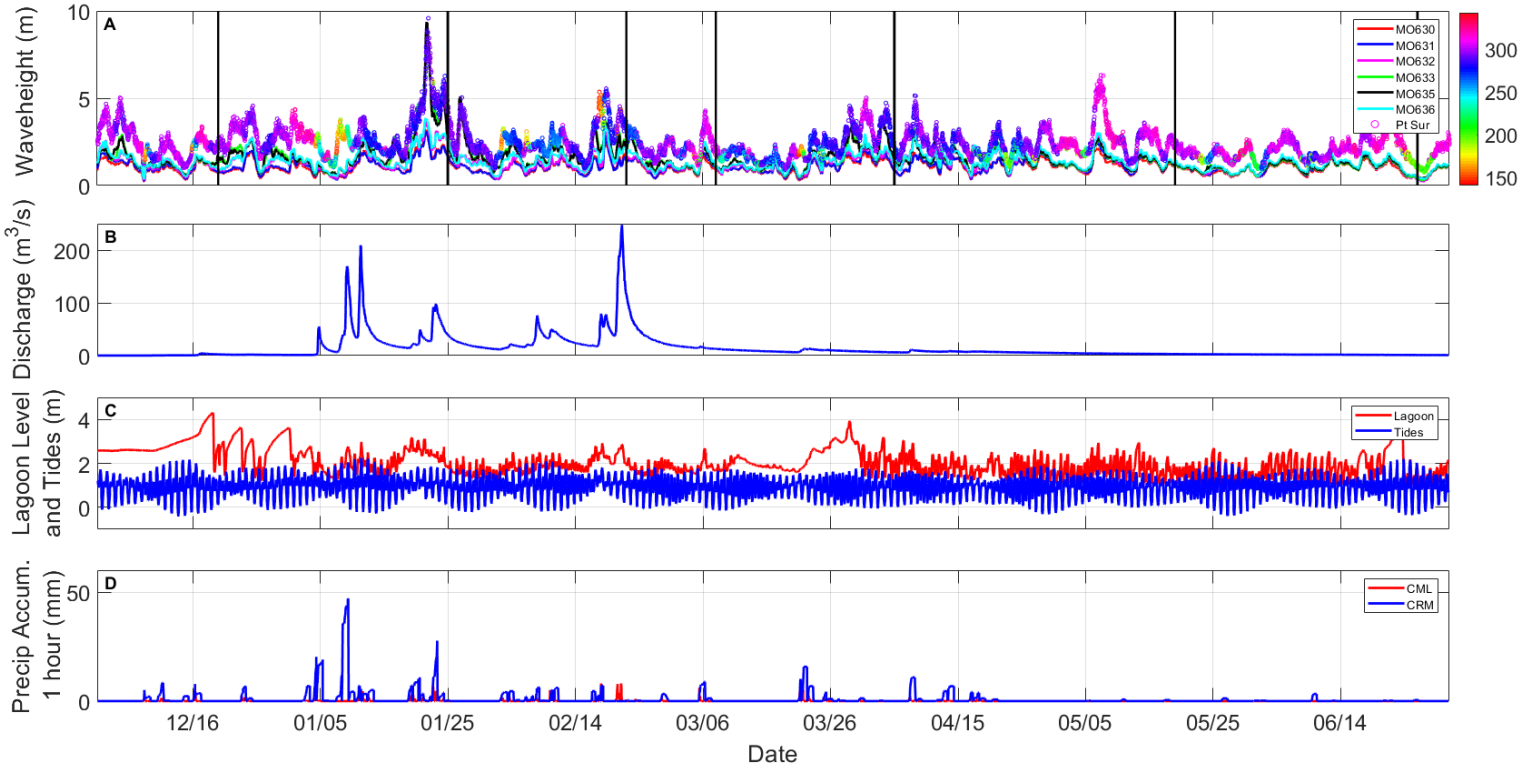

Figure 10. (A) Wave height (m) colored by wave direction, (B) Carmel River discharge (m^3/s), (C) lagoon and tidal water levels (m), and (D) hourly precipitation accumulation (mm) over time from December 1, 2016 to June 30, 2017

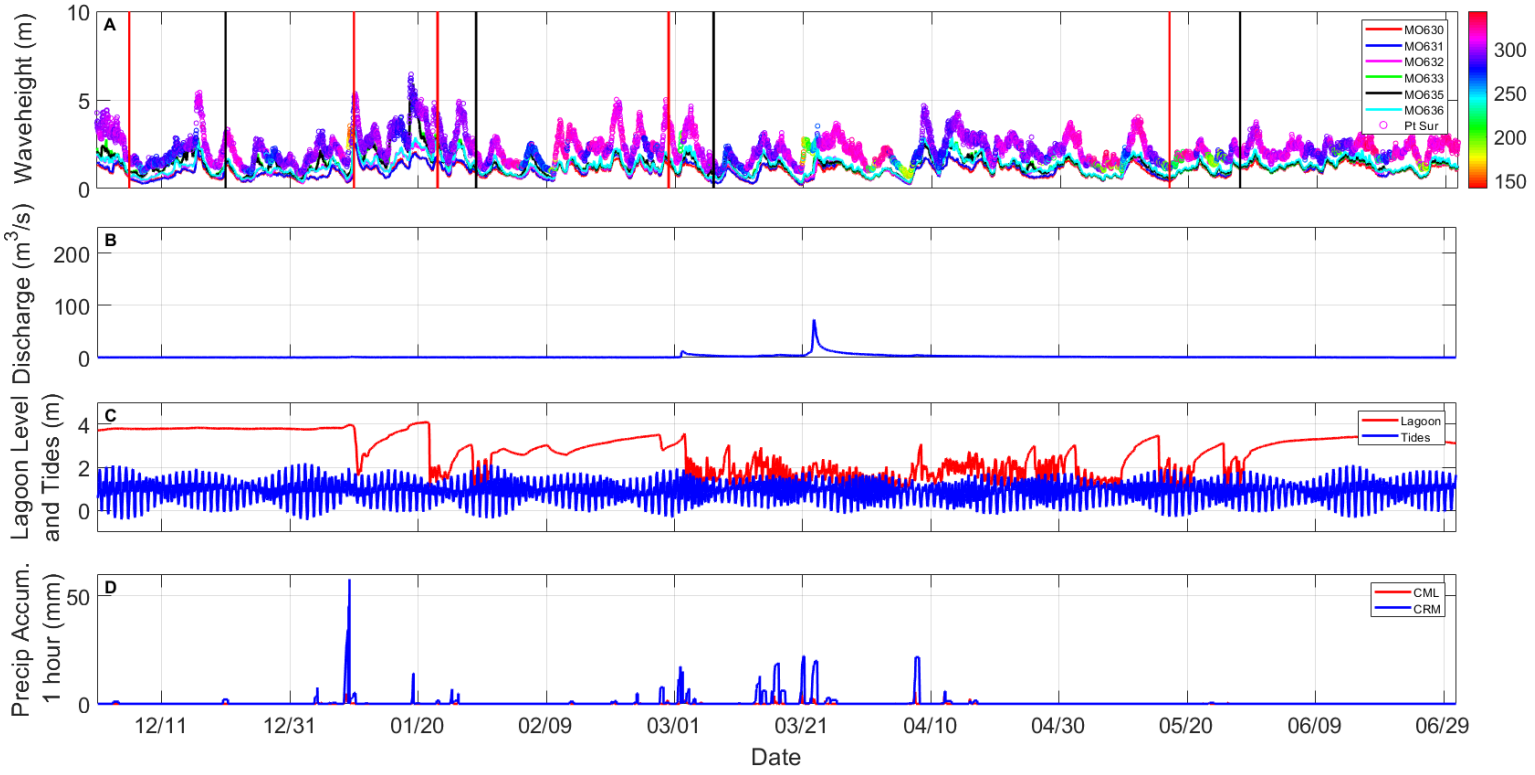

Figure 11. (A) Wave height (m) colored by wave direction, (B) Carmel River discharge (m^3/s), (C) lagoon and tidal water levels (m), and (D) hourly precipitation accumulation (mm) over time from December 1, 2017 to June 30, 2018

3. Wave Height and Direction Comparison

To assess the transport direction of sediment offshore, the alongshore wave height gradient was compared using a northern CDIP MOP site (MO635) and a southern CDIP MOP site (MO632) (Figure 12). This comparison of wave heights along the beachfront yielded stronger differences between the northern and southern location than expected as the MOP sites are located only 160 meters apart (Figure 5). The 2016–2017 breach season experiences the largest height differences with the northern beach receiving larger waves more frequently and for a more prolonged period. Generally, the difference in the wave heights fluctuates around one meter, but is observed to reach a six meter differential along the beach. The periods with the largest wave height differences occur at the end of January.

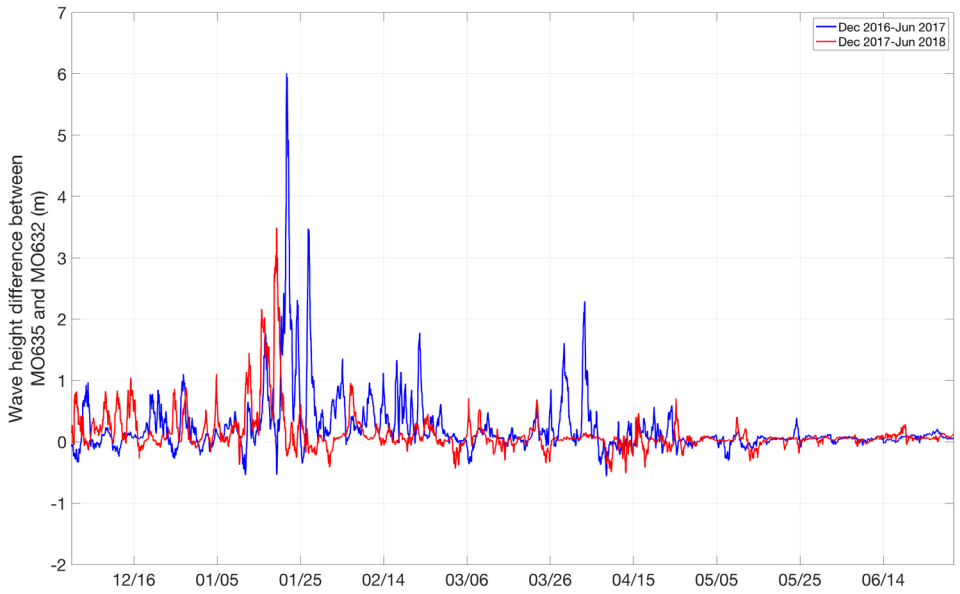

This figure displays wave height differences from December 1, 2016 to June 30, 2017 (blue) and December 1, 2017 to June 30, 2018 (red).

Figure 12. Difference in wave heights (m) between MO635 (north) and MO632 (south)

Wave height differences between offshore and onshore waves (Figure 13) show fairly consistent differences between the waves throughout the breach season. The

average difference between offshore and onshore waves is one meter and is not dependent on offshore wave direction. Similar to the results in Figure 12, the largest differences between the CDIP and Point Sur wave heights exist at the end of January during both seasons. Throughout this period, the majority of the waves appear to come from due west instead of northwest (Figure 14).

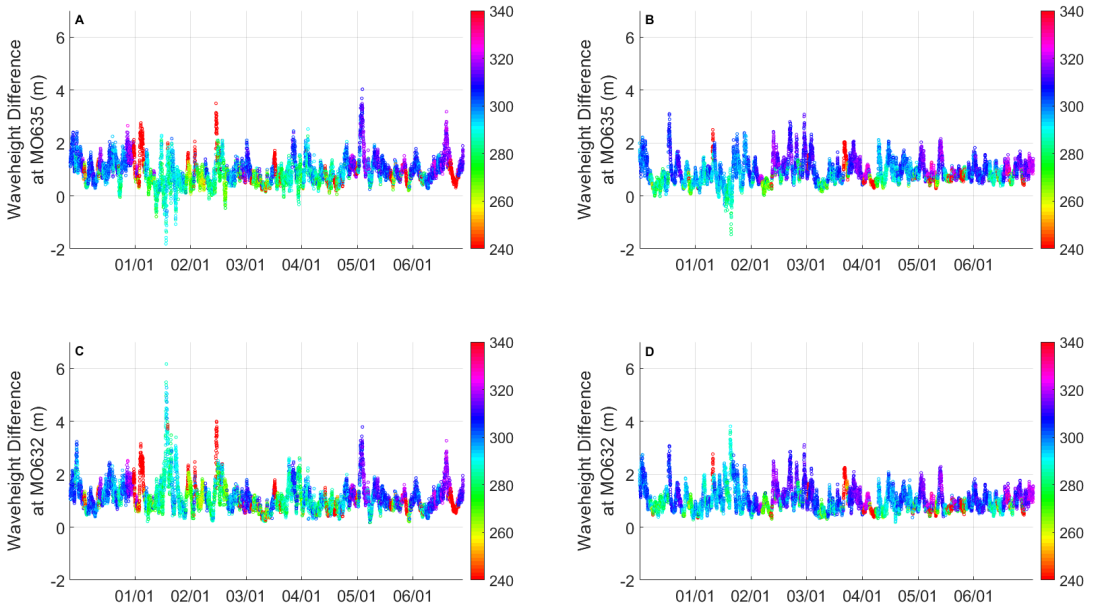

This figure is divided as follows: A) Point Sur minus MO635 from December 2016 – June 2017, B) Point Sur minus MO635 from December 2017 – June 2018, C) Point Sur minus MO632 December 2016 – June 2017, and D) Point Sur minus MO632 from December 2017 – June 2018.

Figure 13. Wave height differences (m) between offshore (Point Sur) buoy data and onshore MOP data colored by wave direction

Wave direction from the six MOP sites display consistent directions throughout the two year study period (Figure 14). However, the direction varies by location suggesting refraction within the basin. Both the extreme northern and southern MOP sites show consistent westerly waves. The MOP sites between these two sites show slight variations in wave direction. MO631 and MO632 show waves from 255–260 degrees while MO633 and MO635 show more southwesterly waves from 245 degrees. These

relative directions are plotted in Figure 14 along with generic radiation stress (S_{xx} and S_{xy}), as discussed in the following section.

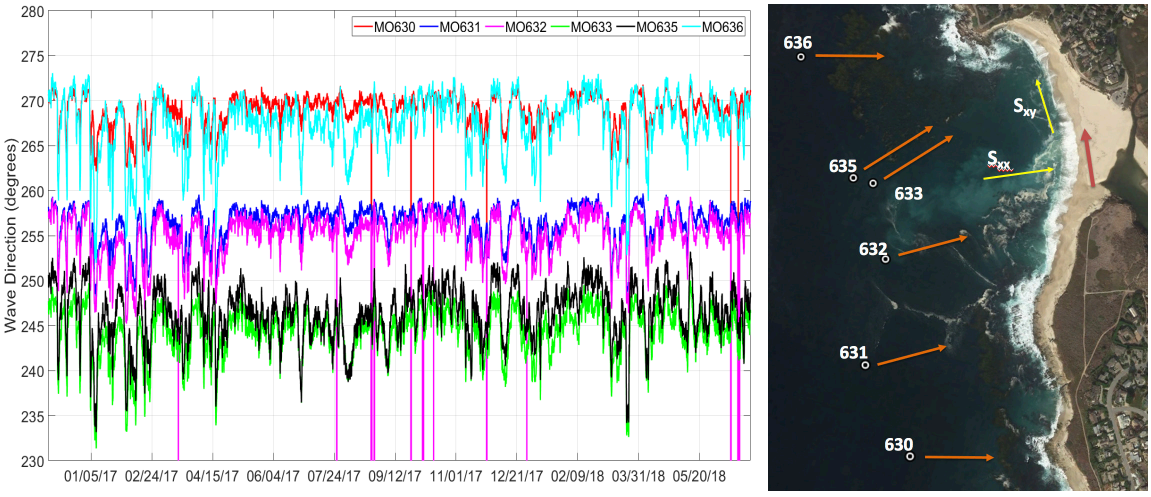

Figure 14. Wave direction at MOP sites along the coast from December 2016 to June 2018 (left); directional schematic along coast (right)

Wave radiation stress is the flux of momentum due to wave action. The cross-shore component (S_{xx}) describes the cross-shore flux of momentum. For this study, all S_{xx} values were found to be positive or onshore as to be expected with shoaling waves. S_{xy} describes the alongshore flux of momentum at the MOP sites (Figure 15). The positive values are in the northern direction while the negative values are in the southern direction. During both seasons, there are northerly radiation stress peaks. The first migratory season experiences stronger S_{xy} values for a prolonged period of time whereas the second season has lower S_{xy} signals. Using these results, alongshore sediment transport is described using the Coastal Engineering Research Center (CERC) equation found in Orzech et al. (2009): $Q_{s,CERC} = KC_bS_{xy}$. In this equation, $Q_{s,CERC}$ is alongshore sediment transport, K is an empirical, dimensional coefficient, and C_b is phase speed at breaking.

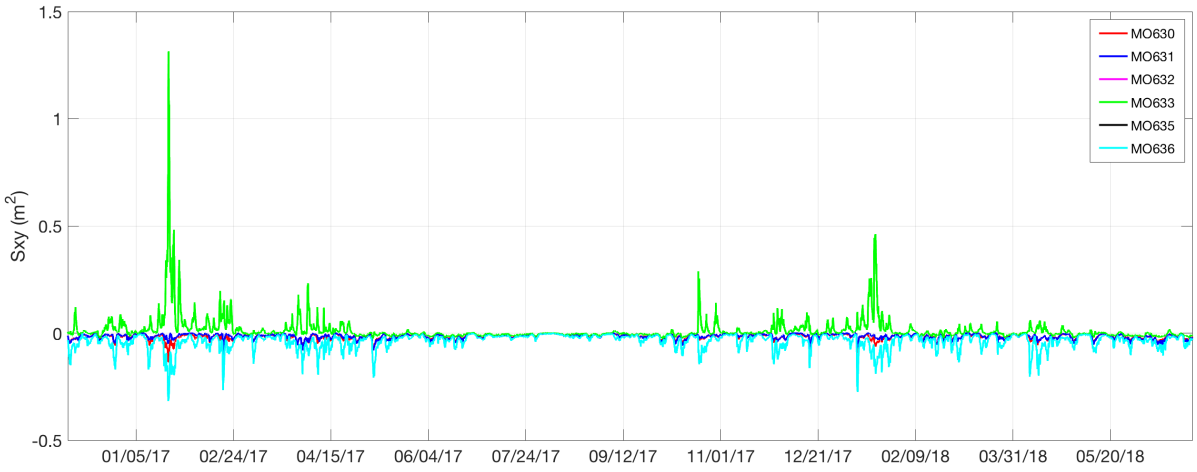

Figure 15. Radiation stress at the MOP sites from December 2016 to June 2018

Table 6. Survey dates and breach locations

Survey Date	Breach Location
12/20/2016	South
01/25/2017	Central, dual outlets
02/22/2017	Central
03/08/2017	North
04/05/2017	South
05/19/2017	South
06/26/2017	South
12/06/2017	Closed
12/21/2017	Closed
01/10/2018	South
01/23/2018	South
01/29/2018	South
02/28/2018	Closed
03/07/2018	South
05/17/2018	South
05/28/2018	South
09/10/2018	Closed

B. DISCUSSION

In Figure 10A, an observable shift in the wave direction occurs from mid-January and through April 2017. This changes the wave direction from northwesterly to predominantly westerly. This shift corresponds with periods when the river breach is open and migrates from the south to the north of the beach (Table 6). Similarly, this wave direction shift is also observed in Figure 11A for the following season. However, in the second season, the shift is not as prolonged as the first year and the change in direction is not as pronounced. The waves shift from 300 degrees to 280–290 degrees and the shift only persists from late December through January. These trends are marked by prolonged northward S_{xy} at MO633, suggesting a net transport of sand northward, that is larger from 2016–2017.

Another key environmental factor is the river discharge rates. During the first season, there are extremely high river discharge flow rates (Figure 10B) for a continued period of time. This high flow occurs while the wave direction is shifted and the river outlet is open and migrating to the north (Table 6). Conversely, the second season saw negligible discharge flow until March (Figure 11B). The variation in discharge flow from the first season to the second suggests that a critical river discharge is necessary to induce migration of the channel.

The wave height gradient of offshore to onshore waves displays an average wave height difference of 1–1.5 meters (Figure 13), supporting the sheltering that occurs within Carmel Bay. An alongshore comparison of wave heights (Figure 12) showed stronger waves to the north of the beach in both breach seasons. During the first season, there is increased northward wave energy for a longer period of time corresponding with the period of westerly waves and breach outlet migration to the north. The second season has stronger waves to the north, but they are not sustained for a prolonged period. During periods of both seasons, the alongshore radiation stress is to the north, and, therefore, northward migration of sediment is expected (Figure 15). The first season has stronger peaks and an extended period of net northerly tendency compared to the second season. As alongshore sediment transport is directly proportional to alongshore momentum flux

(S_{xy}), there is expected an increased northerly sediment transport occurring during the first season (Orzech et al. 2009).

In summary, the 2016–2017 breach season had heavy rain and high river discharge. There was northward directed wave momentum flux and sediment transport via S_{xy} created by the sustained offshore wave direction. The 2017–2018 breach season had less rain and thus minimal river discharge. The alongshore wave momentum and sediment transport was reduced in comparison to the prior year.

THIS PAGE INTENTIONALLY LEFT BLANK

VI. CONCLUSIONS

Due to the migration of the breach, the morphology of CRSB changes yearly, but in a cyclic way that promotes long term stability. During northward breach years, the beach experiences a loss of sediment on the back beach. However, during southward breach years, the back beach gains sediment and can accrete back to its average elevation. These findings demonstrate that there is no net loss or gain of sediment to the system over a long period. This suggests that CRSB is a closed or cyclical system for sediment transport.

This study concludes that the migration of the Carmel River breach outlet is influenced by both the wave climate and the river discharge levels. The wave climate at CRSB shows slight seasonal variations in wave direction, which caused enhanced northward directed wave momentum flux during the first year with prolonged wave direction from the west (rather than northwest). River discharge levels are critical in inducing the migration of the river outlet, where migration was observed during the high flow year and no migration was observed during the low flow year. Due to the extreme differences in river discharge between the two breach seasons in this study, an exact threshold required to induce migration was not established. Future study of seasons with moderate river discharge will be required to ascertain this value. In addition, future studies would benefit from a thorough observation of wave heights to confirm the hindcast estimates from the CDIP MOPs at this site.

Future work at this site could include a historical look into the migratory seasons via data collected by James (2005) to identify and analyze any additional driving factors for river outlet migration. Additionally, an examination of riverine processes and meander thresholds could provide further contributors to the migration pattern of Carmel River. Finally, placing wave buoys in Carmel Bay to observe yearly conditions could establish a more precise local wave climate analysis to further investigate wave effects on breach migration and beach morphology.

The findings in this study demonstrate that SfM is an effective methodology to monitor river outlet migration, net sediment transport, and changes to beach morphology. This suggests that the use of SfM photogrammetry in preparing for future amphibious operations could decrease the cost and time required to scout and survey landing sites. As an example, this study shows that CRSB experiences consistent seasonal sediment transport. This movement effectively decreases sediment cohesion and compaction along the beach, demonstrating that CRSB would not be a successful landing site when moving vehicles or heavy machinery.

LIST OF REFERENCES

Aubrey, D. G. and P. E. Speer, 1984: Updrift migration of tidal inlets. *The Journal of Geology*, **92**, 531–545.

Bascom, W. N., 1953: Characteristics of natural beaches. *Proceedings of 4th Conference on Coastal Engineering*, 163–180.

Behrens D. K., F. A. Bombardelli, J. L. Largier, and E. Twohy, 2009: Characterization of time and spatial scales of a migrating rivermouth. *Geophysical Research Letters*, **36**, https://doi.org/10.1029/2008GL037025.

Behrens, D. K., F. A. Bombarelli, J. L. Largier, and E. Twohy, 2013: Episodic closure of the tidal inlet at the mouth of the Russian River – A small bar-built estuary in California. *Geomorphology*, **189**, 66–80, https://doi.org/10.1016/j.geomorph.2013.01.017

California Irrigation Management Information System (CIMIS), 2008: Station Number 210 Carmel, January 2016-December 2018, California Department of Water Resources, accessed 22 March 2019, https://cimis.water.ca.gov/Default.aspx.

Carrivick J. L., M. W. Smith, D. J. Quincey and S. J. Carver, 2013: Developments in budget remote sensing for the geosciences. *Geology Today*, **29**, 138–143, https://doi.org/10.1111/gto.12015.

Citizen Weather Observation Program (CWOP): Station EW6019, January 2016 – December 2018, accessed 22 March 2019, http://www.wxqa.com/states/CA.html.

Coastal Data Information Program, 2016: MOP v1.1 validation datasets. Accessed 02 April 2019, http://cdip.ucsd.edu/MOP_v1.1/MOP_v1.1_validation.txt.

Coastal Data Information Program: MOP_alongshore, continuing from December 2016 (updated daily), accessed 07 January 2019, https://thredds.cdip.ucsd.edu/thredds/catalog/cdip/model/MOP_alongshore/catalog.html.

Dean, R. G., and R. A. Dalrymple, 2002: *Coastal Processes with Engineering Applications*. Cambridge University Press, 475 pp.

Fonstad, M. A., J. T. Dietrich, B. C. Courville, J. L. Jensen, and P. E. Carbonneau, 2012: Topographic structure from motion: a new development in photogrammetric measurement. *Earth Surface Processes and Landforms*, **38**, 421–430, https://doi.org/10.1002/esp.3366.

Google Earth, Maps showing current and historical Carmel River State Beach and surrounding area (Figure 2), accessed 28 September 2018.

James, G. W., 2005: Surface water dynamics at the Carmel River Lagoon Water Years 1991 through 2005. Monterey Peninsula Water Management Agency, Monterey, Ca.

Jiménez, J., A. H. Sallenger, and L. Fauver, 2007: Sediment transport and barrier island changes during massive overwash events. *Coastal Engineering 2006*, 2870–2879, https://doi.org/10.1142/9789812709554_0242.

Kench, P. S., 1999: Geomorphology of Australian estuaries: Review and prospect. *Australian Journal of Ecology*, **24**, 367–380, https://doi.org/10.1046/j.1442-9993.1999.00985.x.

Komar, P. D., 1998: *Beach Processes and Sedimentation*. R. A. McConnin, Prentice Hall, Inc, 544 pp.

Kraus, N. C., and S. Munger, 2008: Barrier beach breaching from the lagoon side, with reference to Northern California. *Shore & Beach*, **76**, 33–43.

Kraus, N. C., and T. C. Wamsley, 2003: Coastal Barrier Breaching, Part 1: Overview of breaching processes. Coastal and Hydraulics Engineering Technical Note ERDC/CHL CHETN-IV-56, U.S. Army Engineer Research and Development Center, Vicksburg, MS.

Kraus, N. C., A. Militello, and G. Todoroff, 2002: Barrier Breaching Processes and Barrier Spit Breach, Stone Lagoon, California. *Shore & Beach*, **70**.

Monterey Peninsula Water Management District, 2017: WY2017 HWY1 Discharge and Lagoon Water Level. Accessed on 22 March 2019.

Monterey Peninsula Water Management District, 2018: WY2018 HWY1 Discharge and Lagoon Water Levels. Accessed on 11 March 2019.

NOAA NDBC, 2019: Station 46239 Point Sur, CA Historical Data, continuing from December 2016 (updated daily), accessed 07 January 2019, https://www.ndbc.noaa.gov/station_history.php?station=46239.

NOAA Tides and Currents, 2019: NCEP/NOS/CO-OPS Observed Water Levels at 9413450, Monterey, CA, continuing from December 2016 (updated daily), accessed 01 April 2019, https://tidesandcurrents.noaa.gov/waterlevels.html?id=9413450.

Orescanin, M. et al., 2019, *World Scientific*, in press.

Orescanin, M. M. and J. Scooler, 2018: Observations of episodic breaching and closure at an ephemeral river. *Continental Shelf Research*, **166**, 77–82.

Orzech M. D., E. B. Thornton, J. H. MacMahan, W. C. O'Reilly, and T. P. Stanton, 2010: Alongshore rip channel migration and sediment transport. *Marine Geology*, **271**, 278–291, https://doi.org/10.1016/j.margeo.2010.02.022.

Pierce, J. W., 1970: Tidal Inlets and Washover Fans. *The Journal of Geology*, **78**, 230–234.

Rich, A. and E. A. Keller, 2013: A hydrologic and geomorphic model of estuary breaching and closure. *Geomorphology*, **191**, 64–74.

Scooler, J. D., 2017: Episodic changes in lagoon water levels due to ephemeral river breaching and closure events. M.S. thesis, Department of Oceanography, Naval Postgraduate School, 47 pp.

Snavely, N., S. M. Seitz and R. Szeliski, 2008: Modeling the world from internet photo collections. *International Journal of Computer Vision*, **80**, 189–210, https://doi.org/10.1007/s11263-007-0107-3.

Westoby, M. J., J Brasington, N. F. Glasser, M. J. Hambrey and J. M. Reynolds, 2012: 'Structure-from-Motion' photogrammetry: a low-cost, effective tool for geoscience applications. *Geomorphology*, **179**, 300–314, https://doi.org/10.1016/j.geomorph.2012.08.021.

Wolman, M. G., 1967: A cycle of sedimentation and erosion in urban river channels. *Geografiska Annaler, Series A, Physical Geography*, **49**, 385–395, https://doi.org/10.1177/0309133311414527.

Young, W. R., 2018: Sediment Transport associated with ephemeral river breaching and closing events. M.S. thesis, Department of Oceanography, Naval Postgraduate School, 53 pp.

THIS PAGE INTENTIONALLY LEFT BLANK

INITIAL DISTRIBUTION LIST

1. Defense Technical Information Center
   Ft. Belvoir, Virginia

2. Dudley Knox Library
   Naval Postgraduate School
   Monterey, California